



HAL
open science

In situ monitoring of electric field effect on domain wall motion in Co ultrathin films in direct contact with an electrolyte

A. Lamirand, J.-P. Adam, D. Ravelosona, P. Allongue, F. Maroun

► **To cite this version:**

A. Lamirand, J.-P. Adam, D. Ravelosona, P. Allongue, F. Maroun. In situ monitoring of electric field effect on domain wall motion in Co ultrathin films in direct contact with an electrolyte. Applied Physics Letters, 2019, 115 (3), pp.032402. 10.1063/1.5109024 . hal-02324681

HAL Id: hal-02324681


<https://hal.science/hal-02324681v1>

Submitted on 22 Oct 2019

HAL is a multi-disciplinary open access archive for the deposit and dissemination of scientific research documents, whether they are published or not. The documents may come from teaching and research institutions in France or abroad, or from public or private research centers.

L'archive ouverte pluridisciplinaire **HAL**, est destinée au dépôt et à la diffusion de documents scientifiques de niveau recherche, publiés ou non, émanant des établissements d'enseignement et de recherche français ou étrangers, des laboratoires publics ou privés.

AUTHOR QUERY FORM








	<p>Journal: Appl. Phys. Lett.</p> <p>Article Number: 002928APL</p>	<p>Please provide your responses and any corrections by annotating this PDF and uploading it to AIP's eProof website as detailed in the Welcome email.</p>
---	---	--

Dear Author,

Below are the queries associated with your article; please answer all of these queries before sending the proof back to AIP.

Article checklist: In order to ensure greater accuracy, please check the following and make all necessary corrections before returning your proof.

1. Is the title of your article accurate and spelled correctly?
2. Please check affiliations including spelling, completeness, and correct linking to authors.
3. Did you remember to include acknowledgment of funding, if required, and is it accurate?

Location in article	Query / Remark: click on the Q link to navigate to the appropriate spot in the proof. There, insert your comments as a PDF annotation.
<p>AQ1 </p> <p>AQ2 </p>	<p>Please check that the author names are in the proper order and spelled correctly. Also, please ensure that each author's given and surnames have been correctly identified (given names are highlighted in red and surnames appear in blue).</p> <p>Please provide issue number for Ref. 21.</p> <p>Please confirm ORCID's are accurate. If you wish to add an ORCID for any author that does not have one, you may do so now. For more information on ORCID, see https://orcid.org/.</p> <p>A. D. Lamirand - 0000-0003-3016-1377</p> <p>J.-P. Adam </p> <p>D. Ravelosona </p> <p>P. Allongue </p> <p>F. Maroun </p> <hr/> <p>Please check and confirm the Funder(s) and Grant Reference Number(s) provided with your submission:</p> <p>Agence Nationale de la Recherche, Award/Contract Number 16-CE24-0018-04 </p> <p>Please add any additional funding sources not stated above:</p>

Thank you for your assistance.

***In situ* monitoring of electric field effect on domain wall motion in Co ultrathin films in direct contact with an electrolyte**

Cite as: Appl. Phys. Lett. **115**, 000000 (2019); doi: [10.1063/1.5109024](https://doi.org/10.1063/1.5109024)

Submitted: 5 May 2019 · Accepted: 23 June 2019 ·

Published Online: 0 Month 0000



View Online



Export Citation



CrossMark

A. D. Lamirand,^{1,2}  J.-P. Adam,² D. Ravelosona,² P. Allongue,¹ and F. Maroun^{1,a)}

AFFILIATIONS

¹Physique de la Matière Condensée, Ecole Polytechnique, CNRS, IP Paris, 91128 Palaiseau, France

²C2N – CNRS, Université Paris-Sud, Université Paris-Saclay, 91120 Palaiseau, France

^{a)} Author to whom correspondence should be addressed: fouad.maroun@polytechnique.edu

ABSTRACT

We present experimental data on the electric field effect on the magnetic domain wall dynamics in Co ultrathin films in direct contact with an aqueous electrolyte and in the absence of any oxide layer. We use a three electrode electrochemical setup to apply a large and uniform electric field and to precisely separate chemical effects induced by hydrogen from pure electric field effects. We show that in the case of the pure electric field effect, the domain wall velocity varies exponentially with the electric field and that these variations are larger than those observed previously on similar systems due to a larger magnetoelectric coefficient in our case.

Published under license by AIP Publishing. <https://doi.org/10.1063/1.5109024>

Domain wall (DW) motion in perpendicularly magnetized ferromagnets is a field of intensive research.^{1–3} DWs may be displaced by applying an external magnetic field⁴ or by injecting an electric current.^{5–7} In spite of the large current densities required and the associated heat generation and power consumption, the latter process is of the greatest technological relevance since it allows controlling the motion of a larger number of neighboring DWs in racetrack memories³ and addressing individual magnetic nanodevices as memristors.⁸ An elegant approach to reduce the current density and the device power consumption is to lower the magnetic anisotropy energy (MAE) that controls the DW depinning and the motion process. A promising means to achieve this goal is to apply a voltage across an insulating layer between a gate electrode and the ferromagnetic layer to modify the layer MAE.⁹ This method, usually called voltage control of magnetization (VCM), has been widely investigated experimentally and theoretically^{9–11} since the early publication of Weisheit *et al.*¹² More recent studies have demonstrated that magnetic DW velocity in ultrathin films can be modified by the application of a voltage.^{4,13–17}

When considering metallic ferromagnets in contact with an insulating layer, VCM is related to several effects. The first effect is the potential induced accumulation of charges at the ferromagnet surface,^{12,18} which is commonly called the electric field effect (EFE). The second effect is related to the modification of the ferromagnet surface chemistry either by oxidation at the ferromagnet/oxide interface¹⁹ or at the solid/electrolyte contact²⁰ or by molecular adsorption at the

ferromagnet surface in electrolytes.¹⁸ This effect is usually called the magnetoionic effect. The latter process induces large MAE modification reaching several $100 \text{ fJ V}^{-1} \text{ m}^{-1}$, while MAE induced by charge accumulation is generally small (a few $10 \text{ fJ V}^{-1} \text{ m}^{-1}$).⁹

The large majority of the experimental studies has been performed on solid state devices using an insulating layer which may induce chemical modification of the magnetic layer in the presence of an external electric field. Gating directly through an electrolyte, i.e., putting the ferromagnetic layer in direct contact with an electrolyte, is appealing as it prevents possible artifacts induced by the insulating layer and allows the application of larger electric fields.¹² However, the major drawback of this approach is the sample oxidation during its transfer in air between the sample preparation chamber and the cell where magnetic measurements are performed. One alternative approach used by us and others combines *in situ* electrodeposition and magnetic characterization in a single electrochemical cell which avoids transfer of the sample through air.^{18,20–23}

In this work, we investigate the voltage control of MAE and the DW velocity in Co layers in direct contact with an electrolyte and in the absence of any insulating layer using *in situ* magneto-optical Kerr effect (MOKE) imaging of magnetic domains and complementary *in situ* MOKE characterization. We used a specific experimental procedure for contacting Co ultrathin epitaxial layers with an electrolyte *in situ* avoiding any transfer in air and surface oxide formation. In this procedure which was successfully used in recent studies,^{18,21} an

70 ultrathin epitaxial Co layer is grown *in situ* by electrodeposition in the
71 cell used for MOKE measurements. Using this approach, we clearly
72 separate EFE from the magnetoionic effect in an electric field range
73 comparable to that in solid state device studies. We also show that in
74 the case of EFE, the DW velocity varies exponentially with the electric
75 field but with a larger variation coefficient.

76 The Co films (~ 0.8 nm thick) were electrodeposited on a Pd/Au/
77 Si(111) substrate *in situ* in a custom three electrode electrochemical
78 flow cell,^{18,24,25} which was inserted either in the MOKE setup or in the
79 MOKE microscope and connected to a potentiostat. The sample structure
80 and the cell are sketched in the [supplementary material](#) (Fig. S1).
81 The atomically flat Au(111) buffer layers (8 nm thick) were prepared
82 by epitaxial electrodeposition on Si(111).²⁶ The Co layers were covered
83 by a monolayer of carbon monoxide to increase the layer out-of-plane
84 anisotropy and to widen the Co film potential stability range.¹⁸ All
85 magnetic [characterization](#) presented below is conducted under a con-
86 tinuous flow of 0.1 M K_2SO_4 + 1 mM H_2SO_4 + 1 mM KCl saturated
87 with CO. MOKE results on CO covered Co layers deposited on
88 Au/Si(111) samples without a Pd underlayer are given in the [supple-](#)
89 [mentary material](#) for comparison. The polar MOKE setups are home-
90 built and described in previous works and in the [supplementary](#)
91 [material](#).^{18,20,21} The cell is installed vertically between the two poles of
92 an electromagnet, which applies a magnetic field perpendicular to the
93 sample surface. DW velocity v was determined from the traveling dis-
94 tance of the DW during the propagation magnetic pulse averaged over
95 the entire domain.

96 The CO covered Co/Pd/Au/Si(111) samples in contact with the
97 electrolyte are perpendicularly magnetized as demonstrated by square
98 M - H curves with a high coercive field (H_C) measured at different
99 potentials in the range of -0.8 V to -1.3 V [see insets of Fig. 1(a)].
100 The variation of H_C during a potential sweep from -0.8 V to -1.3 V
101 and backward is presented in Fig. 1(a) (open symbols) together with
102 the electrochemical current (solid line). One notices two distinct
103 regimes: for potentials $U > -1$ V, H_C varies quasilinearly with a nega-
104 tive slope, and for $U < -1$ V, H_C decreases, while a significant electro-
105 chemical current starts to flow. This decrease is concomitant with the
106 onset of the electrochemical reaction where H^+ cations in the electro-
107 lyte are transformed into H_2 gas through the hydrogen evolution reac-
108 tion (HER) $2H^+ + 2e^- \rightarrow H_2$.²⁷ Since the observed H_C behavior in
109 the HER regime is quasiabsent in the absence of the Pd underlayer
110 (see the [supplementary material](#), Fig. S3), the prominent decrease in
111 H_C below -1 V observed in Fig. 1(a) suggests that the effect related to
112 HER is specific to the presence of the Pd underlayer.

113 In Fig. 1(b), we present the ratio $\Delta H_C/H_C^0$, the relative variation
114 of H_C with respect to H_C^0 , the value of H_C for $U = -0.8$ V. $\Delta H_C/H_C^0$
115 is plotted as a function of potential measured at different time delays t
116 after the potential step [see the inset in Fig. 1(b)]. The $\Delta H_C/H_C^0$ time
117 transient is composed of an instantaneous jump followed by a slow
118 decay with a time constant τ , before a steady state value is reached (see
119 also Fig. S2). If measured at $t > \tau$ after a potential step (red open sym-
120 bols and red line are guides to the eye), $\Delta H_C/H_C^0$ follows a trend simi-
121 lar to that measured during a potential sweep [Fig. 1(b) black curve],
122 with a maximum around -1.05 V. The results change considerably
123 when considering the values of $\Delta H_C/H_C^0$ acquired immediately after
124 the potential jump [Fig. 1(b) black stars and black line are guides to
125 the eye]. In this case, the variation is almost linear with [time](#) over the
126 entire potential range. By comparison, $\Delta H_C/H_C^0$ is a linear and

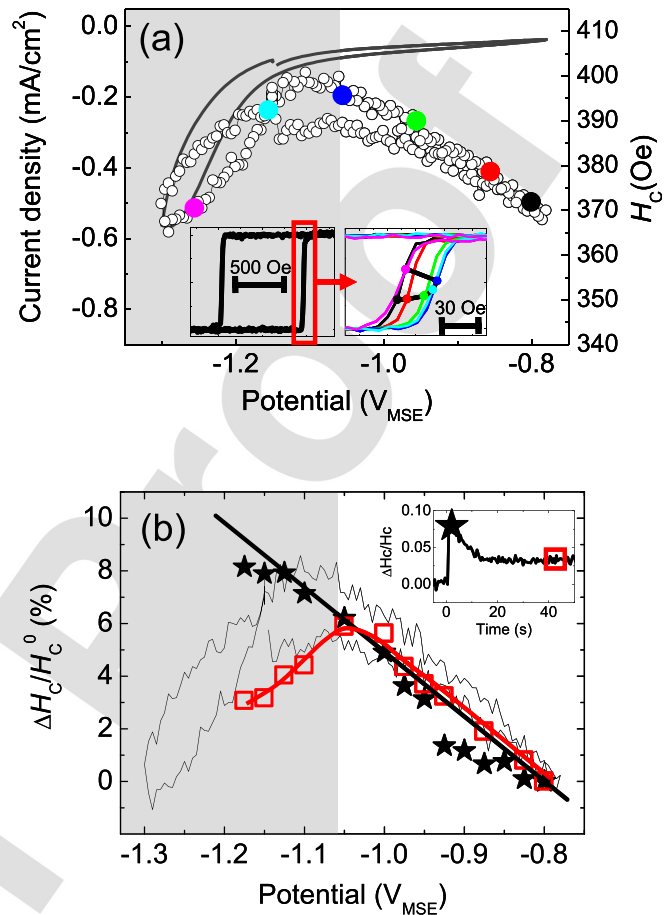


FIG. 1. (a) Potential induced variations of coercive field H_C and electrochemical current upon sweeping the potential at a rate of 20 mV/s. Insets: left, normalized M - H curve of the sample and right, a selection of M - H curves during a potential sweep with a zoom on one edge of the M - H curve. The different colors correspond to various potentials between -0.8 V and -1.3 V. (b) Potential dependence of $\Delta H_C/H_C^0$ measured in steady state conditions (red open squares) or immediately after the application of the potential step (black stars). The black curve corresponds to the potential sweep experiment shown in (a). The black and red lines are guides to the eye. The inset shows $\Delta H_C/H_C^0$ as a function of time during a potential step. The black star and the red square indicate which values are used in the main plots.

reversible function of the applied potential over the same potential
range for CO-covered Co/Au/Si(111) samples in both potential step
and potential sweep experiments (see Fig. S3). Consequently, the effect
induced by the HER may be completely avoided by shortening the resi-
dence time, i.e., the time spent by the sample in this potential range.

We now focus on voltage control of DW velocity (v). Figure 2(a)
presents a typical image of the magnetic domain in Co/Pd/Au/Si(111)
films obtained by polar MOKE microscopy, by subtracting two images
taken after applying the H_{nuc} nucleation pulse and H_{prop} propagation
pulse. The magnetic domain propagates within the dark crown from the
center to the edge (see white arrows). The circular shape of the crown
suggests that the DW propagates isotropically, indicating a rather
homogeneous MAE landscape. The dependence of v as a function of
the propagation field H_{prop} is shown in Fig. 2(b). These measurements

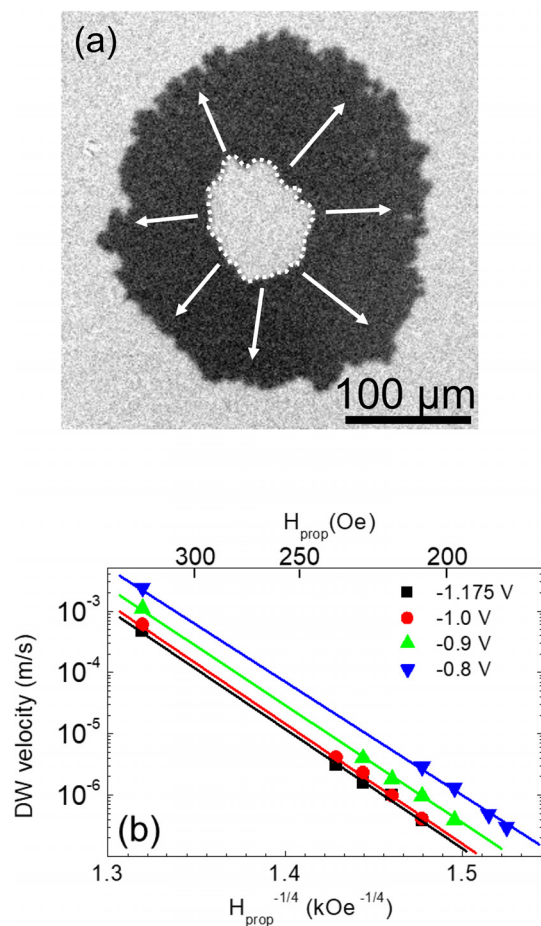


FIG. 2. (a) Example of a “differential” MOKE image of a Co(0.8 nm)/Pd/Au/Si(111) sample after the application of a magnetic field pulse (nucleation 220 Oe during 5 ms, propagation 160 Oe during 2 s) at $U = -0.85$ V to expand an initially formed inverted magnetic domain. (b) Plots of DW velocity as a function of $H_{\text{prop}}^{-1/4}$ (in $\text{kOe}^{-1/4}$) measured at different potentials. For clarity, the top x-axis displays the values of H_{prop} in Oe.

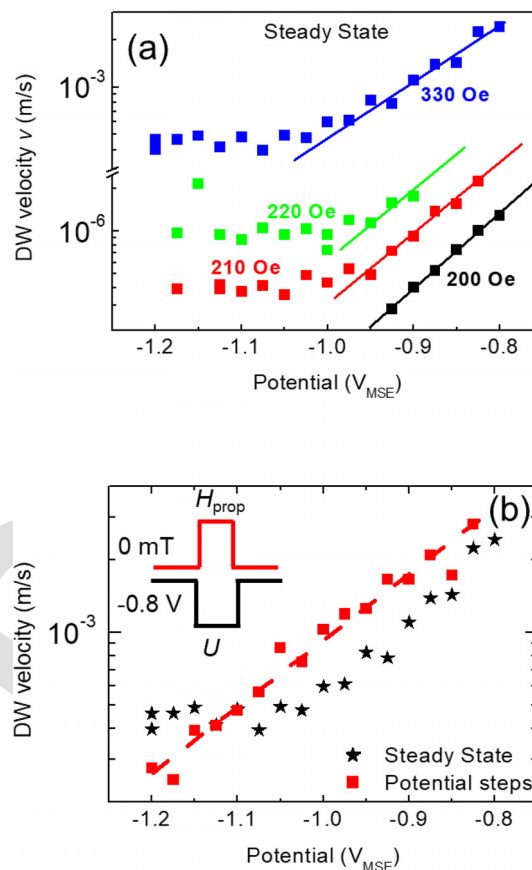


FIG. 3. (a) DW velocity as a function of the potential at different magnetic fields in steady state conditions (where the potential is constant during the entire MOKE image acquisition). A break is introduced along the y-axis to compensate for the rapid increase in v with H_{prop} between 220 and 330 Oe. (b) DW velocity as a function of the potential pulse amplitude at 330 Oe. In this case, all images are recorded at a potential of -0.8 V and the pulses of the field and potential are synchronized as shown in the drawing in the inset. Note the exponential law (red line).

are performed in conditions where the potential is constant during the entire MOKE image acquisition (few seconds). This procedure will be called hereafter steady state conditions. The linear dependence of the logarithm of v as a function of $H_{\text{prop}}^{-1/4}$ indicates that the DW propagation is in the creep regime, i.e., the propagation of the wall is dominated by thermal activation over the energy barrier of pinning sites, and follows the phenomenological equation,⁴

$$v = v_0 \exp\left[-(U_C/kT)(H_{\text{prop}}/H_{\text{dep}})^{-1/4}\right]. \quad (1)$$

In this equation, v_0 is a numerical prefactor, T is the temperature, k is the Boltzmann factor, H_{dep} is the depinning magnetic field, and U_C is the disorder-induced energy barrier arising from the collective pinning of small DW sections. Figure 3(a) presents the dependence of v (on a logarithmic scale) as a function of potential for different values of H_{prop} . For $U > -1$ V, the plots are linear with a slope quasi-independent of H_{prop} . Conversely, for $U < -1$ V, the DW velocity

becomes quasi-independent of the potential, a phenomenon which is concomitant with the regime change of H_C variations observed in Fig. 1(b). These results suggest that H_C and v variations as a function of potential are due to the potential dependence of the Co layer MAE. In order to study v without the influence of the HER, we performed experiments where the residence time at a potential U is short and all MOKE images are acquired at a rest potential of -0.8 V, i.e., outside the HER region. For these experiments, potential and magnetic field pulses are synchronized and last typically 0.2 s. Figure 3(b) presents data measured using this procedure (red squares) together with the steady state measurements (black stars) for a magnetic field of 330 Oe. One clearly observes that using this second procedure v follows an exponential dependence over the full potential range. The slope is slightly different from the one measured in steady state conditions (for $U > -1$ V), and the two plots are slightly shifted. The origin of these differences may probably be a reorganization of the Co surface in contact with the electrolyte, after long steady state measurements over several hours.

173 The polar MOKE and polar MOKE microscopy results clearly
174 show that the more positive the electrochemical potential, the larger
175 the DW velocity and the lower the coercive field. In agreement with
176 our previous studies,¹⁸ this is consistent with a decrease in the MAE at
177 more negative potentials induced by the electric field at the
178 electrolyte/Co interface. In addition to this trend, three main outcomes
179 of this work can be highlighted: (i) *in situ* grown Co layers in contact
180 with an electrolyte present large propagating magnetic domains which
181 can be observed by *in situ* MOKE microscopy, and their DW propaga-
182 tion velocity v follows the creep regime equation in the explored mag-
183 netic field range; (ii) v could be measured at high electric fields (up to
184 3 V/nm) in the absence of an intermediate oxide layer and in the
185 absence of any chemical effect; (iii) v varies exponentially with the
186 applied potential in the absence of chemical effect and becomes quasi-
187 independent of the potential in the HER range. These variations are
188 entirely reversible and take place with a short time constant, corre-
189 sponding to the one of the electrochemical cell we used in this study
190 (20 ms).

191 The first outcome suggests that these electrochemically grown Co
192 films in direct contact with the electrolyte present a low and homoge-
193 neous density of defects as shown in previous *in situ* scanning tunnel-
194 ing microscopy and *in situ* X ray diffraction studies of the Co layer
195 grown on Au(111).^{28,29} These flat Co layers yield a DW propagation
196 regime similar to what is observed in solid state devices prepared by
197 sputtering deposition. It is interesting to note that we obtain v values
198 similar to those for solid state samples with a similar Co thickness and
199 at a H_{prop} value of 250 Oe as AlOx/Co/Pt¹³ and HfO₂/MgO/Co/Pt
200 (after extrapolation to higher magnetic fields).¹⁷

201 The second outcome is directly related to our approach: (i) we
202 grow the ferromagnetic layer *in situ* in an electrochemical environ-
203 ment with the potential control over the sample ensuring that no Co
204 oxide is formed and (ii) the direct contact of the Co layer with the elec-
205 trolyte allows applying large electric fields which are spatially homoge-
206 neous using low applied voltages. This ferromagnetic metal/electrolyte
207 contact with potential control ensures the separation of the pure
208 charge accumulation effect from other effects. In solid state devices,
209 the dielectric layer often interferes in the EFE signal because of electric
210 field induced ion migration and charge trapping in the dielectric layer
211 and surface oxidation of the ferromagnetic layer, leading to slow and
212 often irreversible modifications of the MAE. In our case, potential
213 induced chemical modification of the sample which takes place in the
214 HER regime is well characterized and can be avoided if the potential is
215 applied during short periods.

216 Regarding the last outcome, the exponential dependence of DW
217 velocity v and the linear variations of $\Delta H_C/H_C$ with applied potential
218 are consistent with a linear MAE potential dependence and a pure
219 charge accumulation effect at the electrolyte/Co interface. Indeed, in
220 our previous papers,^{18,21} we demonstrated that the linear behavior of
221 $\Delta H_C/H_C$ is related to a linear change of the electrolyte/Co interface
222 MAE $K_S^{Electrolyte/Co}$. We also showed that whenever electrochemical
223 effects are involved, nonlinear variations of $\Delta H_C/H_C$ are observed as a
224 function of potential.¹⁸ The exponential dependence of v with applied
225 potential linked to a linear modification of the interface anisotropy
226 energy is also consistent with the interpretation given in Ref. 13.

227 We now compare the potential dependence of the velocity for
228 electrolyte/Co/Pd/Au/Si(111) with other studies on solid state devices.
229 In the study of Ref. 13, the influence of the potential on v was

measured at 220 Oe (as in our study), and the range of v as a function
of the propagation field is very similar to that measured in our study.
This suggests that the parameters in the expression of v are also similar
in both cases. To compare quantitatively the potential dependence of
 v , we rewrite the expression governing v in the creep regime,

$$v(E) = v_0 \exp \left[-\alpha(E)(H_{prop})^{-1/4} \right], \quad (2)$$

where E is the electric field and $\alpha = (U_C/kT)(H_{dep})^{1/4}$. Following the
derivation done in Ref. 13, α is proportional to the MAE,

$$\alpha(E) = \alpha_0 \left[K_V + \left(K_S^{Total} + \beta E \right) / d \right], \quad (3)$$

where α_0 contains different micromagnetic parameters of the magnetic
layer, K_V is the Co bulk MAE, $K_S^{Total} = K_S^{Co/Pd} + K_S^{Electrolyte/Co}$,
with $K_S^{Co/Pd}$ being the Co/Pd interface MAE and $K_S^{Electrolyte/Co}$ the
electrolyte/Co interface MAE, d is the layer thickness, and β is the EFE
coefficient, i.e., the variation coefficient per $V\ m^{-1}$ of $K_S^{Electrolyte/Co}$. We
assumed that $K_S^{Electrolyte/Co}$ is linear with the electric field. It is conven-
ient to estimate the electric field difference $\Delta E = E_1 - E_2$ necessary
to increase v by one order of magnitude, the smaller the ΔE , the larger
the EFE. Using Eqs. (2) and (3), we can write

$$v(E_1)/v(E_2) = \exp \left[-\alpha_0(\beta/d)(H_{prop})^{-1/4} \Delta E \right] = 10. \quad (4)$$

The fit of the data in Fig. 2(b) does not allow obtaining a consis-
tent trend in the potential dependence of the parameters governing v .
This is due to the large uncertainty on the fitted slope and offset most
probably because of the small range of available magnetic field. It is
therefore more accurate to use the potential dependence of v measured
at a fixed magnetic field. From the fit of the data in the exponential
regime in Fig. 3(a) and considering that the distance between the
charged planes responsible for the EFE is ~ 0.14 nm (see Fig. S1),²¹ we
obtain $\Delta E \sim 1.5$ V/nm. In the case of AlOx/Co/Pt, the AlOx thickness
is 3.8 nm and the data reported in Ref. 13 yield $\Delta E \sim 4$ V/nm.
Consequently, the EFE is 2.7 times larger in our case as compared to
Ref. 13. This is related to one of the parameters inside the exponential
term. The cobalt thickness d and H_{prop} are similar in both studies. The
parameter α_0 should be also similar for both systems since the mea-
sured DW velocity is similar for similar H_{prop} . Consequently, the dif-
ference should come from the β coefficient. In our case, β equals
34 fJ $V^{-1} m^{-1}$,¹⁸ whereas it amounts to 14 fJ $V^{-1} m^{-1}$ for AlOx/Co/
Pt,¹³ i.e., 2.4 times smaller, a value very close to that obtained above,
2.7. This indicates that the higher EFE measured in our case is essen-
tially due to the higher value of the parameter β in our work. The dif-
ference between the two systems may originate from the orbital shape
of the Co atoms which are bonded to the carbon atoms of the CO
overlayer in our case and to oxygen in the case of the AlOx/Co inter-
face. The comparison with HfO₂/MgO/Co/Pt is less straightforward
because v at 220 Oe is two orders of magnitude larger than in our
case.¹⁷ In addition, the value of β in this study is very large (~ 150 fJ
 $V^{-1} m^{-1}$), well above the range of 10–50 fJ $V^{-1} m^{-1}$ of β values usu-
ally measured for Co and CoFeB layers,^{30–34} which suggests that
chemical processes might be involved.

In steady-state conditions and in the HER region, i.e., at poten-
tials between -1 V and -1.3 V, the DW velocity levels off and deviates
from the exponential law, suggesting the presence of a second effect on

MAE with the opposite sign compensating the EFE. In the CO saturated electrolyte, this second regime exists only in the presence of the Pd underlayer and is concomitant with significant changes of the sample reflectivity (see Fig. S4). Since it was previously observed that Pd reflectivity changes upon H-insertion/release,³⁵ we infer that this second effect on MAE is connected with the insertion and removal of atomic hydrogen in and out of the Pd layer. Magnetic studies of Co/Au(111) layers capped with Pd clearly show that H loading into Pd modifies the Co MAE.³⁵ A similar phenomenon can be expected in our case, provided that the H can reach the Pd underlayer, either by diffusion through the Co layer or directly in the Pd layer through pinholes in the Co layer.

The magnetic domains of electrodeposited perpendicularly magnetized Co epitaxial layers were imaged by MOKE microscopy, while the sample surface is oxide-free and in contact with an electrolyte. The domain walls propagate in the creep regime, and the velocity varies exponentially with the potential (slope ~ 2.5 decades/V). The exponential variation originates from the linear variations of the surface anisotropy energy with potential (i.e., charge accumulation at the surface), and a quantitative comparison with literature suggests that the slope scales with the parameter β used to characterize the efficiency of the electric field effect on MAE, which is ~ 2.5 larger at the electrolyte/Co than at the AlOx/Co interface. In the steady state condition and at potential where HER settles in, the DW velocity levels off, probably due to hydrogen incorporating in the Pd underlayer.

See the [supplementary material](#) for complete experimental details and additional magnetic and reflectivity results of Co/Pd/Au/Si(111) and Co/Au/Si(111) samples.

This work was supported by two public grants from the French National Research Agency (ANR): Labex NanoSaclay, reference: ANR-10-LABX-0035, and ELECSPIN ANR-16-CE24-0018-04.

313 REFERENCES

- 314 ¹C. Chappert, A. Fert, and F. N. Van Dau, *Nat. Mater.* **6**(11), 813–823 (2007).
- 315 ²D. A. Allwood, G. Xiong, C. C. Faulkner, D. Atkinson, D. Petit, and R. P. Cowburn, *Science* **309**(5741), 1688–1692 (2005).
- 316 ³S. S. P. Parkin, M. Hayashi, and L. Thomas, *Science* **320**(5873), 190–194 (2008).
- 317 ⁴P. J. Metaxas, J. P. Jamet, A. Mougou, M. Cormier, J. Ferré, V. Baltz, B. Rodmacq, B. Dieny, and R. L. Stamps, *Phys. Rev. Lett.* **99**(21), 217208 (2007).
- 318 ⁵M. Tsoi, R. E. Fontana, and S. S. P. Parkin, *Appl. Phys. Lett.* **83**(13), 2617–2619 (2003).
- 319 ⁶D. Ravelosona, S. Mangin, J. A. Katine, E. F. Eric, and B. D. Terris, *Appl. Phys. Lett.* **90**(7), 072508 (2007).

- 320 ⁷C. Burrowes, A. P. Mihai, D. Ravelosona, J. V. Kim, C. Chappert, L. Vila, A. Marty, Y. Samson, F. Garcia-Sanchez, L. D. Buda-Prejbeanu, I. Tudosa, E. E. Fullerton, and J. P. Attane, *Nat. Phys.* **6**(1), 17–21 (2010).
- 321 ⁸S. Lequeux, J. Sampaio, V. Cros, K. Yakushiji, A. Fukushima, R. Matsumoto, H. Kubota, S. Yuasa, and J. Grollier, *Sci. Rep.* **6**, 31510 (2016).
- 322 ⁹B. Dieny and M. Chshiev, *Rev. Mod. Phys.* **89**(2), 025008 (2017).
- 323 ¹⁰D. Chun-Gang, P. V. Julian, R. F. Sabirianov, Z. Ziqiang, C. Junhao, S. S. Jaswal, and E. Y. Tsybal, *Phys. Rev. Lett.* **101**(13), 137201 (2008).
- 324 ¹¹K. Nakamura, R. Shimabukuro, T. Akiyama, T. Ito, and A. J. Freeman, *Phys. Rev. B* **80**(17), 172402 (2009).
- 325 ¹²M. Weisheit, S. Fahler, A. Marty, Y. Souche, C. Poinsignon, and D. Givord, *Science* **315**(5810), 349–351 (2007).
- 326 ¹³A. J. Schellekens, A. van den Brink, J. H. Franken, H. J. M. Swagten, and B. Koopmans, *Nat. Commun.* **3**, 847 (2012).
- 327 ¹⁴A. Bernard-Mantel, L. Herrera-Diez, L. Ranno, S. Pizzini, J. Vogel, D. Givord, S. Auffret, O. Boule, I. M. Miron, and G. Gaudin, *Appl. Phys. Lett.* **102**(12), 122406 (2013).
- 328 ¹⁵U. Bauer, S. Emori, and G. S. D. Beach, *Appl. Phys. Lett.* **100**(19), 192408–192404 (2012).
- 329 ¹⁶H. Kakizakai, K. Yamada, M. Kawaguchi, K. Shimamura, S. Fukami, N. Ishiwata, D. Chiba, and T. Ono, *Jpn. J. Appl. Phys., Part 1* **52**, 070206 (2013).
- 330 ¹⁷D. Chiba, M. Kawaguchi, S. Fukami, N. Ishiwata, K. Shimamura, K. Kobayashi, and T. Ono, *Nat. Commun.* **3**, 888 (2012).
- 331 ¹⁸N. Tournerie, A. P. Engelhardt, F. Maroun, and P. Allongue, *Phys. Rev. B* **86**(10), 104434 (2012).
- 332 ¹⁹F. Bonell, Y. T. Takahashi, D. D. Lam, S. Yoshida, Y. Shiota, S. Miwa, T. Nakamura, and Y. Suzuki, *Appl. Phys. Lett.* **102**(15), 152401 (2013).
- 333 ²⁰N. Di, J. Kubal, Z. Zeng, J. Greeley, F. Maroun, and P. Allongue, *Appl. Phys. Lett.* **106**(12), 122405 (2015).
- 334 ²¹N. Tournerie, A. Engelhardt, F. Maroun, and P. Allongue, *Surf. Sci.* **631**, 88–95 (2015).
- 335 ²²K. Leistner, N. Lange, J. Hänisch, S. Oswald, F. Scheiba, S. Fähler, H. Schlörb, and L. Schultz, *Electrochim. Acta* **81**(Suppl. C), 330–337 (2012).
- 336 ²³K. Duschek, M. Uhlemann, H. Schlörb, K. Nielsch, and K. Leistner, *Electrochim. Commun.* **72**(Suppl. C), 153–156 (2016).
- 337 ²⁴P. Allongue, F. Maroun, H. F. Jurca, N. Tournerie, G. Savidand, and R. Cortes, *Surf. Sci.* **603**, 1831–1840 (2009).
- 338 ²⁵P. Allongue and F. Maroun, *MRS Bull.* **35**(10), 761–770 (2010).
- 339 ²⁶P. Prod'homme, F. Maroun, R. Cortes, and P. Allongue, *Appl. Phys. Lett.* **93**(17), 171901 (2008).
- 340 ²⁷J. O. M. Bockris and A. K. N. Reddy, *Modern Electrochemistry* (Plenum Press, New York, 1977), Vol. 2.
- 341 ²⁸C. A. Lucas, F. Maroun, N. Sisson, P. Thompson, Y. Gründer, R. Cortès, and P. Allongue, *J. Phys. Chem. C* **120**(6), 3360–3370 (2016).
- 342 ²⁹N. Di, A. Damian, F. Maroun, and P. Allongue, *J. Electrochem. Soc.* **163**(12), D3062–D3068 (2016).
- 343 ³⁰W.-G. Wang, M. Li, S. Hageman, and C. L. Chien, *Nat. Mater.* **11**, 64 (2012).
- 344 ³¹S. Kanai, M. Yamanouchi, S. Ikeda, Y. Nakatani, F. Matsukura, and H. Ohno, *Appl. Phys. Lett.* **101**(12), 122403 (2012).
- 345 ³²M. Endo, S. Kanai, S. Ikeda, F. Matsukura, and H. Ohno, *Appl. Phys. Lett.* **96**(21), 212503 (2010).
- 346 ³³U. Bauer, S. Emori, and G. S. D. Beach, *Appl. Phys. Lett.* **101**(17), 172403–172404 (2012).
- 347 ³⁴W. W. Lin, N. Vernier, G. Agnus, K. Garcia, B. Ocker, W. S. Zhao, E. E. Fullerton, and D. Ravelosona, *Nat. Commun.* **7**, 13532 (2016).
- 348 ³⁵F. Maroun, F. Reikowski, N. Di, T. Wiegmann, J. Stettner, O. M. Magnussen, and P. Allongue, *J. Electroanal. Chem.* **819**, 322–330 (2018).

AQ2